

# Photoenhanced Heterogeneous Uptake of NO<sub>2</sub> and HONO Formation on Authentic Winter Time Urban Grime

Chuan Yu, Liubin Huang,\* Likun Xue,\* Hengqing Shen, Zeyuan Li, Min Zhao, Juan Yang, Yingnan Zhang, Hongyong Li, Jiangshan Mu, and Wenxing Wang\*



Cite This: *ACS Earth Space Chem.* 2022, 6, 1960–1968



Read Online

ACCESS |



Metrics & More



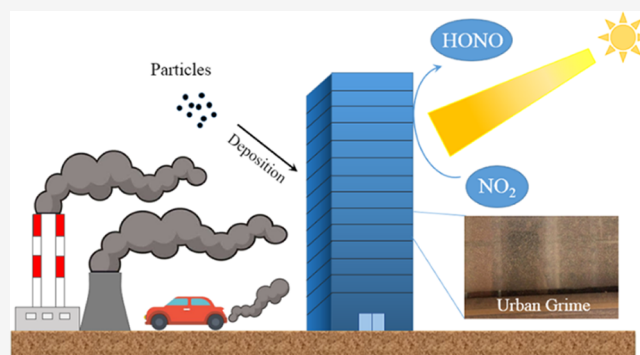
Article Recommendations



Supporting Information

**ABSTRACT:** Heterogeneous reactions of NO<sub>2</sub> on surfaces seem to be an important sink for NO<sub>2</sub> and a source for HONO in the atmosphere. Although heterogeneous reactions of NO<sub>2</sub> have been extensively investigated in laboratory studies, kinetic data about this reaction on real ambient surfaces are limited. Therefore, in the present study, we investigated the heterogeneous reaction of NO<sub>2</sub> on urban grime, representative of surface film in urban areas, under various experimental conditions using a Teflon box system. The role that light played in these reactions was also explored. It was found that the uptake coefficient ( $\gamma$ ) of NO<sub>2</sub> and HONO yield both were significantly enhanced under UV conditions, which was consistent with the literature results. The  $\gamma$  of NO<sub>2</sub> on urban grime increased linearly with the increasing light intensity, whereas the yield of HONO seemed to be independent of the light intensity. In addition to the intensity of light, heterogeneous reactions of NO<sub>2</sub> on urban grime were also significantly affected by the initial concentration of NO<sub>2</sub> and relative humidity. On the basis of the data measured, the flux of HONO production from photoenhanced NO<sub>2</sub> uptake on urban grime was calculated to be  $(3.8\text{--}10.0) \times 10^9$  molecules cm<sup>-2</sup> s<sup>-1</sup>. This result suggests an important role of urban grime in the daytime NO<sub>2</sub>-to-HONO conversion and could be helpful to explain unknown daytime HONO sources in polluted urban areas.

**KEYWORDS:** heterogeneous reaction, nitrogen dioxide, urban grime, nitrous acid, uptake coefficient



## INTRODUCTION

Nitrous acid (HONO) is of great significance in atmospheric chemistry. It is well known as an important precursor of the OH radical, which plays a critical role in the oxidation capacity of the atmosphere.<sup>1–4</sup> The reaction of gaseous NO with OH radicals is the major daytime source of HONO, whereas the heterogeneous reaction of NO<sub>2</sub> on wet particles is recognized as the dominant pathway in the nighttime.<sup>5–8</sup> However, recent field studies observed the unexpected high concentration of HONO during daytime hours that cannot be explained by the well-accepted gas-phase oxidation pathways or direct vehicle emissions, suggesting the existence of unknown daytime sources of HONO.<sup>9,10</sup> Given the strong active photochemistry in the daytime, photolysis of HNO<sub>3</sub> and nitrate on the surfaces of particles, ground, or leaves was proposed to be the potential source.<sup>11–14</sup> Additionally, heterogeneous reactions of NO<sub>2</sub> on various surfaces (e.g., humic acid, polycyclic aromatic hydrocarbons (PAHs), mineral dust, and soot) under irradiation were also examined.<sup>15–27</sup> Compared to dark conditions, the reactivity of NO<sub>2</sub> was found to be significantly promoted under irradiation. The uptake coefficient ( $\gamma$ ) of NO<sub>2</sub> measured in the presence of light is 1 or 2 orders of magnitude higher than that in the absence of light.<sup>22,28,29</sup> Since HONO is one of the

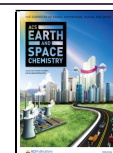
important products during the reaction, the significant enhancement of HONO formation is also observed along with the uptake of NO<sub>2</sub>. Therefore, in addition to nighttime, heterogeneous reactions of NO<sub>2</sub> may also be of great importance in daytime chemistry for HONO formation. However, it is found that previous studies on the photoreaction of NO<sub>2</sub> were mostly focused on pure chemicals or simple proxies instead of ambient surfaces. Impurity in particles could alter the behaviors of heterogeneous NO<sub>2</sub> uptake and HONO formation. Liu et al.<sup>27</sup> reported that the presence of Na<sub>2</sub>SO<sub>4</sub> can significantly diminish the  $\gamma$  of NO<sub>2</sub> and HONO yield in the heterogeneous reaction of NO<sub>2</sub> with pure fluorene. The photoenhanced  $\gamma$  of NO<sub>2</sub> showed a linear positive relation with relative humidity (RH) on humic acid particles, but it increased at first and then decreased with increasing RH on the mixture of humic acid and benzophenone particles.<sup>17,30</sup> Therefore, it is essential to investigate the heterogeneous

Received: February 21, 2022

Revised: June 13, 2022

Accepted: June 13, 2022

Published: June 24, 2022



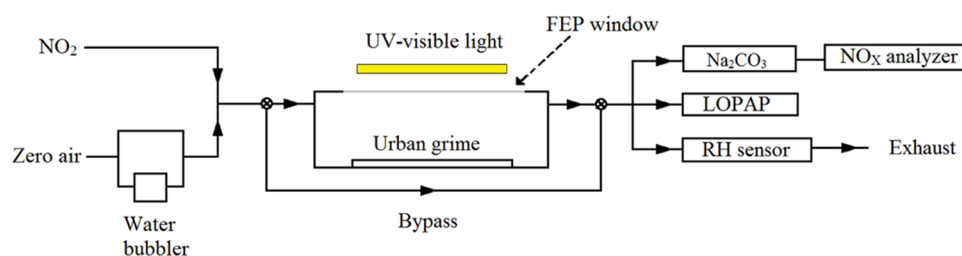


**Figure 1.** Schematic diagram of the Teflon box reactor system.

reaction of  $\text{NO}_2$  on atmospheric relevant particles or surfaces; however, kinetic data about these reactions is scarce.

In urban areas, it is noted that urban surfaces (e.g., buildings, roadways, and sidewalks) can also provide a medium for the reactions of atmospheric trace gases similar to suspended particles. Via deposition and chemical processes, a film of a complex mixture of organic and inorganic materials, which is usually referred to as urban grime or environmental film, can also be formed on urban surfaces.<sup>31–35</sup> A model study revealed that the surface area provided by the ground surface was comparable to that of atmospheric particles,<sup>36,37</sup> suggesting the potential importance of the heterogeneous reaction of  $\text{NO}_2$  on urban grime. A recent study has reported the photoenhanced uptake of  $\text{NO}_2$  and HONO production on real urban grime, with  $\gamma$  of  $(1.1–5.8) \times 10^{-6}$  at <1 to 90% RHs.<sup>38</sup> Our previous work has investigated the heterogeneous reaction of  $\text{NO}_2$  on urban grime collected in Hong Kong, China, exploring effects of light and RH on  $\gamma$  of  $\text{NO}_2$  as well as the yield of HONO formation.<sup>29</sup> However, it is noted that urban grime is a complex mixture of species, so different emission characteristics in different locations may alter the chemical compositions of urban grime.<sup>31,32,39–45</sup> Therefore, the heterogeneous behavior of  $\text{NO}_2$  on more kinds of urban grime under different conditions should be investigated to better quantify the roles of these processes in HONO production and urban air quality.

Therefore, in this study, a series of experiments were further performed to investigate the heterogeneous reactions of  $\text{NO}_2$  on urban grime, which was collected in north China during the heating season, using a Teflon box reactor. The photoenhanced heterogeneous uptake of  $\text{NO}_2$  and HONO formation on urban grime were presented and the influence of experimental conditions (i.e.,  $\text{NO}_2$  concentration, light intensity, and RH) was explored. The results obtained are helpful in understanding the important role of urban grime in the daytime  $\text{NO}_2$ -to-HONO conversion.

## EXPERIMENTAL SECTION

**Apparatus.** Experiments of heterogeneous reactions of  $\text{NO}_2$  on urban grime were carried out in a flow reactor system. The schematic diagram of the reactor system is shown in Figure 1. The reactor consists of a Teflon box (inner size of 30 cm  $\times$  12 cm  $\times$  5 cm) with a 30 cm  $\times$  12 cm fluorinated ethylene propylene (FEP) window on the top. Urban grime samples were collected by placing 27 cm  $\times$  10 cm quartz glass plates on an open balcony on the second floor of a building in downtown Qingdao, Shandong Province (36.08°N, 120.39°E) during the heating season from December 10, 2020, to January 10, 2021. The weight of urban grime collected was  $\sim$ 0.016 g. The heating season is a period of winter time (from November 15 to March 15 of the next year) in North China Plain for residential heating. Coal is the most common residential heating fuel in urban areas of China. More details about the

experimental apparatus and sample preparation can be seen in our previous study.<sup>29</sup> Experiments were carried out at room temperature ( $\sim$ 295 K) and different RHs in the dark or under UV irradiation. UV-vis light (18 W, Arcadia Products Plc., U.K.) was used to generate light, and light intensity was controlled by the number of lamps. Spectral irradiance was measured by a Spectro-Radiometer (Specbos 1211UV, JETI Technische Instrumente GmbH, Germany), and the light spectrum is shown in Figure S1. The photolysis frequency of  $\text{NO}_2$  was measured by a CCD spectrometer (PFS-100, Focused Photonics (Hangzhou) Inc., China) to assess the interference of  $\text{NO}_2$  photolysis on these processes. RH was controlled by adjusting the relative flow rate of zero air (free of  $\text{NO}_x$ ,  $\text{O}_3$ ,  $\text{SO}_2$ , CO, and hydrocarbons), which was generated by a zero air supplier (Model 111, Thermo Fisher Scientific), passing through a water bubbler to the total airflow. The exact value of RH was also monitored by an RH probe (RH-USB, Omega). Prior to experiments, a quartz glass plate with urban grime was placed in the reactor. A gas flow containing  $\text{NO}_2$  (10 ppmv standard gas, Qingdao Weierda Gas) was diluted with zero air before entering the reactor. The total 3 LPM gas flow was alternatively directed through either bypass or box reactor via valves. The  $\text{NO}_2$  concentration in the total flow was  $\sim$ 20 to 135 ppbv. The residence time of air in the box reactor was calculated to be 36 s. In blank experiments, a clean glass plate was placed in the reactor instead of the glass plate with urban grime to obtain blank results.

**Detection of Reactants and Products.** The  $\text{NO}_2$  concentration was measured by a chemiluminescence analyzer with a molybdenum converter (Model 42i, Thermo Fisher Scientific) coupled to a sodium carbonate denuder (60 cm  $\times$  1 cm id Teflon tube). The sodium carbonate denuder was used to remove HONO in the gas phase, which could lead to an overestimation in the measurement of  $\text{NO}_2$  by an analyzer. The HONO concentration was measured by a long-path absorption photometer (LOPAP-03, QUMA, Germany) that has been applied in several studies.<sup>46–50</sup> The detailed description can be found in Heland et al.<sup>51</sup> Briefly, it is based on wet chemical sampling and photometric detection. HONO is absorbed by sulphanilamide–hydrochloric acid solution in a sampling unit. And then, the resulting solution is mixed with naphthylethylenediamine–dihydrochloride solution and subsequently converted to an azo dye. The azo dye is pumped into a detection unit consisting of a long tube, and the absorption spectra are measured to calculate the HONO concentration.

Amounts of metal in urban grime were analyzed by an inductively coupled plasma mass spectrometer (ICP-MS, Agilent 7700, Agilent Technologies Inc.). Urban grime was scraped off from the sample plate and subsequently predigested in 7 mL of aqua regia and 1 mL of  $\text{H}_2\text{O}_2$  (298 K) for 30 min. And then, the suspension was digested by

microwave digestion at 120 °C for 60 min, 180 °C for 60 min, and 220 °C for 60 min. After that, the resulting solution was injected into ICP-MS to measure the concentrations of 10 metal elements (Al, Ca, Cu, Fe, Mg, Mn, Pb, Ti, V, and Zn).

In addition to metal elements, concentrations of polycyclic aromatic hydrocarbons (PAHs) in urban grime were also measured. Urban grime was scraped off from the sample plate and then extracted for 30 min sonication twice using 5 mL of acetonitrile saturated with the *n*-hexane solution. The extract was filtered and the resulting solution containing PAHs was analyzed by a gas chromatograph equipped with a mass spectrometer (GC-MS, TRACE 1300-ISQ LT, Thermo Fisher Scientific). The carrier gas was high-purity helium with a flow velocity of 0.7 mL min<sup>-1</sup>. The column temperature was held at 80 °C for 2 min, heated to 180 °C for 5 min at a rate of 10 °C min<sup>-1</sup>, and then heated to 300 °C for 5 min at a rate of 5 °C min<sup>-1</sup>.

**Determination of the Uptake Coefficient and the Yield.** In this study, the uptake of NO<sub>2</sub> on urban grime was assumed to be a pseudo-first-order reaction, thus rate constant (*k*) of this reaction can be expressed by eq E1

$$k = \ln \left( \frac{[\text{NO}_2]_0}{[\text{NO}_2]_t} \right) / t \quad (\text{E1})$$

where [NO<sub>2</sub>]<sub>0</sub> is the initial concentration of NO<sub>2</sub>, ppbv; [NO<sub>2</sub>]<sub>t</sub> is the NO<sub>2</sub> concentration measured at the exit of the reactor, ppbv; and *t* is the resident time of NO<sub>2</sub> in the reactor, s. On the basis of the pseudo-first-order reaction assumption, the uptake coefficient (*γ*) of NO<sub>2</sub> can be calculated using eq E2

$$\gamma = \frac{4(k_p - k_b)}{\omega(S/V)} \quad (\text{E2})$$

where *k<sub>p</sub>* and *k<sub>b</sub>* are the rate constants of NO<sub>2</sub> on urban grime or on clean glass (blank experiment), s<sup>-1</sup>; respectively; *ω* is the mean molecular velocity, m s<sup>-1</sup>; *V* is the volume of the reactor, m<sup>3</sup>; and *S* is the surface area of the quartz glass plate, m<sup>2</sup>. Accordingly, all *γ* calculated in this study represent the geometric uptake coefficient of NO<sub>2</sub>.

Additionally, the yield and flux of HONO during the processes were also estimated. The yield of HONO production (*Y<sub>HONO</sub>*), defined as the ratio of the net concentration of the formed HONO to the net concentration of the consumed NO<sub>2</sub> (eq E3), was also calculated.

$$Y^{\text{HONO}} = \frac{[\Delta\text{HONO}]_p - [\Delta\text{HONO}]_b}{[\Delta\text{NO}_2]_p - [\Delta\text{NO}_2]_b} \quad (\text{E3})$$

where [ΔHONO]<sub>p</sub> and [ΔNO<sub>2</sub>]<sub>p</sub> are concentrations of HONO generated and NO<sub>2</sub> consumed from NO<sub>2</sub> uptake on urban grime, respectively, ppbv; [ΔHONO]<sub>b</sub> and [ΔNO<sub>2</sub>]<sub>b</sub> are concentrations of HONO generated and NO<sub>2</sub> consumed from NO<sub>2</sub> uptake on the clean glass plate, ppbv.

The flux of HONO production from urban grime was calculated by eq E4

$$\text{flux} = \frac{([\Delta\text{HONO}]_p - [\Delta\text{HONO}]_b)fP}{RAT S} \quad (\text{E4})$$

where *f* is the total flow rate of the reagent gas, m<sup>3</sup> s<sup>-1</sup>; *P* is the ambient pressure, Pa; *R* is the gas constant, J mol<sup>-1</sup> K<sup>-1</sup>; *T* is the ambient temperature, K; *A* is Avogadro's constant; and *S* is the surface area of the quartz glass plate, m<sup>2</sup>.

## RESULTS AND DISCUSSION

### Photoenhanced NO<sub>2</sub> Uptake and HONO Formation.

Each experiment was conducted with the following experimental procedures as shown in Figure 2. First, the air was

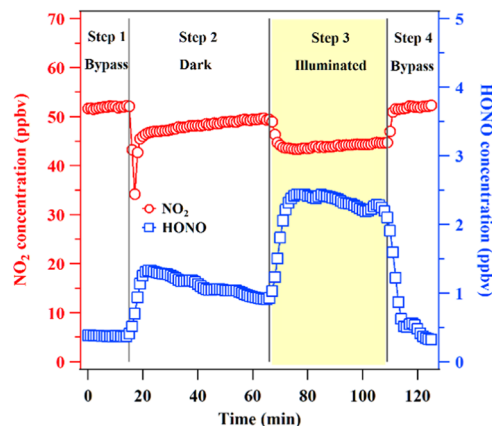


**Figure 2.** Temporal changes of NO<sub>2</sub> and HONO concentration during the NO<sub>2</sub> uptake experiment. Experimental conditions: UV–vis light irradiation of 5.2 W m<sup>-2</sup>, initial NO<sub>2</sub> concentration of 52.2 ppbv, and RH of 64%. Red circles and blue squares represent the concentration of NO<sub>2</sub> and HONO, respectively.

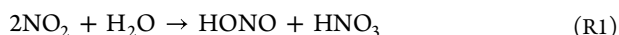
switched to bypass to measure the initial NO<sub>2</sub> concentration (step 1). When the initial NO<sub>2</sub> concentration was stable, the flow was switched back to pass through the box reactor to react with urban grime in the dark for ~60 min (step 2). It was noted that HONO was the potential product formed during the reaction, thus, in addition to NO<sub>2</sub>, the concentration of HONO was also monitored at the exit of the box reactor. And then, the lamp was turned on to investigate the effects of irradiation on the heterogeneous reactions of NO<sub>2</sub> with urban grime (step 3). After the reaction, the lamp was turned off and NO<sub>2</sub> was bypassed from the reactor to measure the concentration again (step 4). Figure 2 displays how the NO<sub>2</sub> and HONO concentrations changed during these processes when the sample was exposed to NO<sub>2</sub> in the dark or under irradiation. In some experiments, a clean glass plate was placed in the reactor to run the same procedures to obtain the blank results (Figure S2).

As shown in Figure 2, in the absence of light, when NO<sub>2</sub> was just introduced into the reactor, its concentration rapidly decreased within 3 min first and then gradually increased until a steady-state condition was achieved (step 2). The steady *γ* value of NO<sub>2</sub> was calculated as  $(0.51 \pm 0.12) \times 10^{-6}$ . This value is higher than that reported in our previous study, which also determined the *γ* value of NO<sub>2</sub> on urban grime collected in Hong Kong, China, under dark conditions.<sup>29</sup> Because the same measurement method was employed, this discrepancy may be partly attributed to the different components of urban grime collected at different sites. Several studies have reported that the chemical composition of urban grime varies at different times or in different locations.<sup>31,32,39,45</sup> In this study, the sample was collected during the heating season. The higher *γ* value indicates that urban grime collected in Qingdao during the heating season could be more reactive to NO<sub>2</sub> compared to urban grime collected in Hong Kong, China. When the lamp was turned on, it was found that the NO<sub>2</sub> concentration started to decrease again (step 3), from ~49 to ~43 ppbv. Analogously, we also calculated the *γ* value after the NO<sub>2</sub>



concentration approached a plateau under irradiation. This value  $[(1.52 \pm 0.04) \times 10^{-6}]$  is 3 times larger than that under dark conditions, suggesting the significant role that light plays in the heterogeneous reaction of  $\text{NO}_2$  on urban grime.

Figure 2 also shows the decrease in the  $\text{NO}_2$  concentration with the concomitant formation of HONO. The yield of HONO formation was calculated as 24% in the absence of light. The possible mechanism for HONO formation is elucidated via  $\text{NO}_2$  hydrolysis as shown in reaction R1.<sup>7</sup>

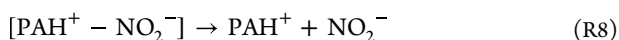
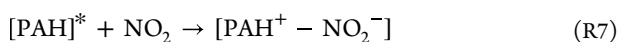


Under irradiation, it is noted that HONO yield is also enhanced similar to the  $\gamma$  value. The increment of HONO yield suggests that there exist additional pathways for HONO formation. The photoenhanced  $\text{NO}_2$  uptake and HONO yield have also been observed on other kinds of surfaces, such as  $\text{Fe}_2\text{O}_3$ ,  $\text{TiO}_2$ , and polycyclic aromatic hydrocarbons (PAHs).<sup>19–21,27,52–54</sup>  $\text{TiO}_2$  is well known as a photosensitizer.<sup>55,56</sup> When  $\text{TiO}_2$  is excited by light, an electron in the conduction band and a hole in the valence band can be formed (R2). The electron can react with adsorbed  $\text{NO}_2$  to form  $\text{NO}_2^-$ , facilitating the conversion of  $\text{NO}_2$  and thereby promoting the uptake of  $\text{NO}_2$  (R4). The formed  $\text{NO}_2^-$  subsequently combined with  $\text{H}^+$ , resulting in the formation of HONO (R5).



$\text{Fe}_2\text{O}_3$  is also a ubiquitous photosensitizer. Heterogeneous uptake of  $\text{NO}_2$  on  $\alpha\text{-Fe}_2\text{O}_3$  shows an enhancement under UV irradiation as well, yielding reduced nitrogen species on the surface of  $\alpha\text{-Fe}_2\text{O}_3$ .<sup>54</sup>

Analogous to  $\text{TiO}_2$  and  $\text{Fe}_2\text{O}_3$ , the enhancement of the  $\text{NO}_2$  uptake on PAH particles under irradiation is also attributed to the promotion of  $\text{NO}_2$  conversion on the surface; however, the detailed mechanism is different.<sup>19–21,27</sup> PAHs can get excited by irradiation, and then the electronically excited state of PAHs combines with  $\text{NO}_2$  to form a  $[\text{PAH}^+ - \text{NO}_2^-]$  complex via the electron transfer pathway. The complex then decomposes into  $\text{PAH}^+$  and  $\text{NO}_2^-$  (R8). HONO is produced through the combination of  $\text{NO}_2^-$  and  $\text{H}^+$ .



During the heating season, large amounts of metals including Fe and Ti<sup>57–60</sup> as well as organics including PAHs<sup>61–64</sup> can be emitted along with the particulate matter. Table S1 lists concentrations of different metal elements in urban grime. The concentration of Fe and Ti in urban grime was measured as  $31.38 \pm 5.17$  and  $0.53 \pm 0.07 \text{ mg g}^{-1}$ , respectively. In addition to metal elements, concentrations of PAHs in urban grime were also measured as shown in Table S2. 16 PAHs were detected in urban grime with a total

concentration of  $4.04 \pm 0.28 \mu\text{g g}^{-1}$ . Therefore, the significant increase in the  $\gamma$  value and HONO yield under irradiation observed in this study can be partially ascribed to the presence of  $\text{TiO}_2$ , iron oxides, or PAH components in the collected urban grime. However, it is noted that the concentration of Fe and Ti is at least 2 orders of magnitude higher than that of PAHs, thus it seems that the enhancement of  $\text{NO}_2$  uptake as well as HONO yield under irradiation is mainly contributed by metal oxides rather than PAHs. Additionally, in consideration of the complexity of the composition of urban grime, the presence of other potential pathways responsible for HONO formation cannot be excluded. Further investigation on the products of  $\text{NO}_2$  uptake on urban grime is warranted for a comprehensive understanding of the reaction mechanism.

**Influence of Experimental Conditions.** As mentioned above, the uptake of  $\text{NO}_2$  by urban grime can be significantly enhanced in the presence of light. Thus, the effects of light intensity on this process were examined. Figure 3 shows a

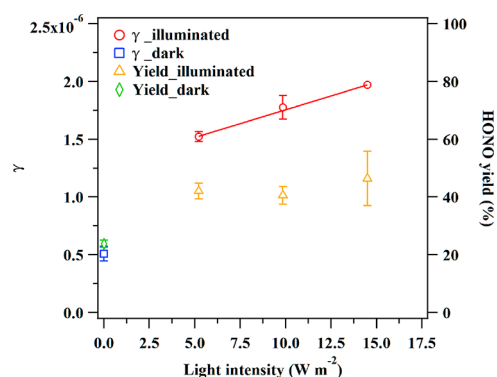


**Figure 3.** Uptake coefficients of  $\text{NO}_2$  and HONO yield on urban grime as a function of the light intensity, at an initial  $\text{NO}_2$  concentration of 52.2 ppbv and RH of 64%. The red circles, blue squares, yellow triangles, green diamond symbols, and error bars represent the average values of  $\gamma$  under UV–vis light and dark conditions and the average values of HONO yield under UV–vis light and dark conditions, and standard deviation, respectively.

linear increase in  $\gamma$  with the increasing light intensity. The dependence of photoenhanced  $\gamma$  on light intensity can be described using eq E5

$$\gamma = (4.8 \pm 0.4) \times 10^{-8} \times [\text{light intensity}] (\text{W m}^{-2}) + (1.3 \pm 0.1) \times 10^{-6} \quad (\text{E5})$$

To the best of our knowledge, no study has investigated the influence of light intensity on  $\text{NO}_2$  uptake on authentic urban grime. Nevertheless, a similar linear dependence on light intensity has been found in PAHs,<sup>19–21,27</sup> humic acid,<sup>17</sup> humic acid + benzophenone,<sup>30</sup> and soot particles.<sup>26</sup> For example, Han et al.<sup>17</sup> reported that  $\gamma$  ranged from  $(1.67 \pm 0.14) \times 10^{-6}$  under  $68.5 \text{ W m}^{-2}$  to  $(4.37 \pm 0.45) \times 10^{-6}$  under  $195 \text{ W m}^{-2}$  on humic acid particles at 30 ppbv  $\text{NO}_2$  and 22% RH. Although the  $\gamma$  value increases with the increasing light intensity, it seems that HONO yield is independent of light intensity (Figure 3). This observation is also consistent with the result of a previous study that investigated the influence of light intensity on the yield of HONO produced from the heterogeneous reaction of  $\text{NO}_2$  on humic acid.<sup>17</sup> However, the HONO yield measured in the present study is much lower than that in their study (74%). This value is 1.7 times higher

than the HONO yield measured in our study (43%). It is noted that nonvolatile products, such as nitrate and nitrite, can also be formed in the heterogeneous reactions of  $\text{NO}_2$  with particles in addition to HONO. The discrepancy in the HONO yield between urban grime and humic acid suggests that urban grime may be prone to form nonvolatile products.

In addition to light intensity, we also investigated the effects of  $\text{NO}_2$  concentration on the uptake of  $\text{NO}_2$  and HONO formation. Figure 4 displays the change of  $\gamma$  and HONO yield

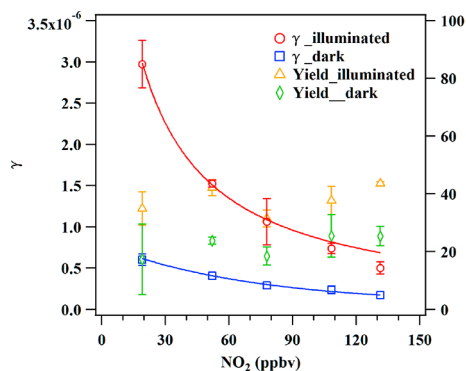


**Figure 4.** Uptake coefficients of  $\text{NO}_2$  and HONO yields on urban grime as a function of  $\text{NO}_2$  concentration, under UV–vis light irradiation of  $5.2 \text{ W m}^{-2}$  and at 64% RH. The red circles, blue squares, yellow triangles, and green diamond symbols and error bars represent the average values of  $\gamma$  under UV–vis light and dark conditions, the average values of HONO yield under UV–vis light and dark conditions, and standard deviation, respectively.

as a function of  $\text{NO}_2$  concentration in the absence and presence of light. When the  $\text{NO}_2$  concentration increased from 19 ppbv to 131 ppbv,  $\gamma$  decreased from  $(0.60 \pm 0.07) \times 10^{-6}$  to  $(0.17 \pm 0.02) \times 10^{-6}$  in the dark and decreased from  $(2.97 \pm 0.29) \times 10^{-6}$  to  $(0.50 \pm 0.07) \times 10^{-6}$  under irradiation. These results suggest that the uptake of  $\text{NO}_2$  on urban grime is less efficient at higher  $\text{NO}_2$  concentrations both under irradiation and dark. The dependence of photoenhanced  $\gamma$  on the initial  $\text{NO}_2$  concentration under irradiation can be empirically described using eq E6

$$\gamma = \frac{1}{(9.9 \pm 1.3) \times 10^3 \times [\text{NO}_2](\text{ppbv}) + (1.4 \pm 0.3) \times 10^5} \quad (\text{E6})$$

Previous studies also proposed that the increase in  $\text{NO}_2$  concentration can significantly inhibit the uptake of  $\text{NO}_2$  on various kinds of particles (e.g., PAHs, humic acid, mineral dust, and soot).<sup>17,19–22,24,26,27</sup> The Langmuir–Hinshelwood mechanism is usually used to explain such an inverse dependence.<sup>19,21,22,27,30</sup>  $\text{NO}_2$  is first adsorbed on the surface of urban grime through gas-particle phase partitioning and then proceeds in the reactions with reactive species. Thus, the inverse dependence was attributed to the saturation of available adsorption sites. Although  $\text{NO}_2$  uptake is negatively dependent on the initial  $\text{NO}_2$  concentration, it is expected that HONO yield was rarely influenced by  $\text{NO}_2$  concentration, which is consistent with the observation of previous studies.<sup>17,19–21,30</sup>

The influences of RH on  $\text{NO}_2$  uptake on urban grime under dark and UV conditions are shown in Figure 5. The uptake of  $\text{NO}_2$  on urban grime is significantly enhanced at higher RH both under dark and UV conditions compared to lower RH.

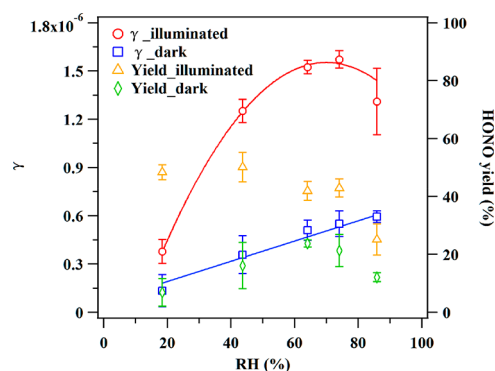


**Figure 5.** Uptake coefficients of  $\text{NO}_2$  and HONO yields on urban grime as a function of RH under UV–vis light irradiation of  $5.2 \text{ W m}^{-2}$  and at an initial  $\text{NO}_2$  concentration of 52.2 ppbv. The red circles, blue squares, yellow triangles, green diamond symbols, and error bars represent the average values of  $\gamma$  under UV–vis light and dark conditions, the average values of HONO yield under UV–vis light and in dark conditions, and standard deviation, respectively.

However, the trend of  $\gamma$  value for RH dependence is different between these experimental conditions. In the dark,  $\gamma$  linearly increase with the increasing RH. This may be ascribed to the hydrolysis of  $\text{NO}_2$  on wet surfaces.<sup>7</sup> Similar trend has also been found for urban grime collected in Hong Kong, China.<sup>29</sup> It is noted that there exists an inflection point under irradiation.  $\gamma$  also increases from  $(0.38 \pm 0.07) \times 10^{-6}$  at 18% RH to  $(1.57 \pm 0.05) \times 10^{-6}$  at 74% RH at first, but then dropped to  $(1.31 \pm 0.21) \times 10^{-6}$  at 86% RH. The dependence of photoenhanced  $\gamma$  on RH under irradiation can be empirically described using eq E7

$$\gamma = -(4.4 \pm 0.9) \times 10^{-10} \times ([\text{RH}] (\%))^2 + (6.2 \pm 0.8) \times 10^{-8} \times [\text{RH}] (\%) - (6.1 \pm 1.8) \times 10^{-7} \quad (\text{E7})$$

As mentioned above, the chemical conversion of  $\text{NO}_2$  on urban grime may mainly occur via three pathways under irradiation: (1) reacting with surface active sites, (2) reacting with the photoinduced oxidants (e.g., electron and trigger excited radicals), or (3) reacting with surface adsorbed water (i.e., hydration). Adsorbed water can occupy surface active sites and consequently inhibit the photoreaction of surface species, but it can also accelerate  $\text{NO}_2$  hydration. Moreover, it is noted that adsorbed water can decompose into two OH radicals under irradiation, providing the additional pathway for  $\text{NO}_2$  conversion.<sup>24,52</sup> Therefore, the increase in  $\gamma$  with the increasing RH requires that the role of adsorbed water in the promotion of  $\text{NO}_2$  uptake prevails over its inhibition effects. Previous studies observed that the amount of water vapor uptake onto urban grime has a positive relation with RH (0–75%),<sup>13,43</sup> indicating that more water is accumulated on urban grime at higher RH. Consequently, the amount of adsorbed water or the hygroscopicity of urban grime significantly affects the trend of  $\text{NO}_2$  uptake dependent on RH. This is also the possible explanation for the different inflection points observed on various kinds of particles (e.g.,  $\text{TiO}_2$ , Arizona Test Dust, humic acid, and humic acid mixed with benzophenone).<sup>24,28,52</sup> For example, inflection point occurred at 15% RH on  $\text{TiO}_2$  particles,<sup>52</sup> but occurred at 22% RH on humic acid mixed with benzophenone.<sup>28</sup> Moreover, a linear dependence of  $\gamma$  on RH was found on urban grime collected in south China under UV light.<sup>38</sup> This discrepancy may also be the result of the different

composition, particle size, and hygroscopicity properties of urban grimes.

The change in the HONO yield as a function of RH is also investigated. Figure 5 shows that there exists an inflection point at ~62% RH for HONO yield in the dark. The presence of water can promote the hydrolysis of NO<sub>2</sub> as shown in R1, resulting in higher HONO production. Furthermore, the adsorbed H<sub>2</sub>O can also contribute to the H<sup>+</sup> transfer to generate HONO from nitrites formed on the surface.<sup>18</sup> However, with the increase in RH, the adsorbed H<sub>2</sub>O can also compete with NO<sub>2</sub> for the surface active sites, resulting in a decrease in HONO yield along with  $\gamma$ . Baergen and Donaldson investigated the direct photolysis of urban grime and found that HONO formation increased as the RH increased to 35%, then plateaued, and even slightly decreased with further increase in RH.<sup>13</sup> This indicates that urban grime might be deliquescent and form water film at high RH, thereby preventing the release of HONO. This may be also the possible explanation for the observation of the decrease in the HONO yield at a higher RH. The HONO yield was reported as 28% at 5% RH and 46% at 70% RH on urban grime collected in Hong Kong, China under irradiation.<sup>29</sup> The yield in this study is in good agreement with that at ~70% RH but higher than that at low RH. This discrepancy can be attributed to the differences in the chemical composition and hygroscopicity property in urban grime in Qingdao or Hong Kong, China.

## ■ ATMOSPHERIC IMPLICATION AND CONCLUSIONS

In this study, we investigated the heterogeneous reaction of NO<sub>2</sub> on urban grime collected in north China during the heating season. Under irradiation, NO<sub>2</sub> shows a much stronger reactivity to urban grime compared to dark conditions, resulting in higher HONO generation. The photoenhanced HONO formation via NO<sub>2</sub> uptake could further influence the oxidation capacity of the urban atmosphere given that it serves as the important reservoir for OH radicals.<sup>1–4,65</sup> On the basis of data collected, the flux of HONO was estimated using eq E4. Table 1 summarizes the results of HONO flux calculated at different experimental conditions, ranging from  $3.8 \times 10^9$  to  $10.0 \times 10^9$  molecules cm<sup>-2</sup> s<sup>-1</sup>. The daytime missing sources of HONO have been found in north China in several studies.<sup>66,67</sup> Spataro et al.<sup>67</sup> reported an average daytime missing source of 2.58 ppbv h<sup>-1</sup> for the HONO formation rate in Beijing. Tang

**Table 1. Flux of HONO Production on Urban Grime at Different Scenarios**

experimental conditions			flux of HONO production (molecules cm <sup>-2</sup> s <sup>-1</sup> )
NO <sub>2</sub> (ppbv)	RH (%)	light intensity (W m <sup>-2</sup> )	
52.2	86	5.2	(4.2 ± 0.3) × 10 <sup>9</sup>
52.2	74	5.2	(8.7 ± 0.9) × 10 <sup>9</sup>
52.2	64	5.2	(8.1 ± 0.4) × 10 <sup>9</sup>
52.2	44	5.2	(8.8 ± 0.8) × 10 <sup>9</sup>
52.2	18	5.2	(3.8 ± 1.2) × 10 <sup>9</sup>
52.2	64	9.8	(7.6 ± 0.7) × 10 <sup>9</sup>
52.2	64	14.5	(10.0 ± 1.5) × 10 <sup>9</sup>
19.2	64	5.2	(4.8 ± 0.4) × 10 <sup>9</sup>
77.9	64	5.2	(6.3 ± 0.1) × 10 <sup>9</sup>
108.4	64	5.2	(7.6 ± 1.4) × 10 <sup>9</sup>
131.4	64	5.2	(7.0 ± 1.1) × 10 <sup>9</sup>

et al.<sup>66</sup> reported that this value could be up to 2.5 ppbv h<sup>-1</sup> in the north China plain (Beijing–Tianjin–Hebei region). To calculate the HONO source strength from urban grime in urban areas, the urban surface–volume ratio (*S/V*) should be obtained. Typically, the *S/V* value was set as 0.1–0.3 m<sup>-1</sup> in previous model studies.<sup>68–70</sup> Here, a middle value of 0.2 m<sup>-1</sup> was used, and the formation rate of HONO contributed by urban grime was accordingly estimated to be 1.1–2.7 ppbv h<sup>-1</sup> in the atmosphere. The calculated result was comparable to the reported missing source in north China, indicating that NO<sub>2</sub> uptake on urban grime could be an important pathway for daytime HONO formation in urban areas and should be considered in current atmospheric chemical models. Moreover, our results showed that the photoenhanced HONO production on urban grime collected in Qingdao ( $3.8–10.0 \times 10^9$  molecules cm<sup>-2</sup> s<sup>-1</sup>) was 2 times larger than that of urban grime collected in Hong Kong, China ( $1.9–5.3 \times 10^9$  molecules cm<sup>-2</sup> s<sup>-1</sup>).<sup>29</sup> Further investigation is still needed to study the reactivity of NO<sub>2</sub> on urban grime collected from different locations to better quantify the contribution of such heterogeneous reaction to the HONO source strength.

## ■ ASSOCIATED CONTENT

### Supporting Information

The Supporting Information is available free of charge at <https://pubs.acs.org/doi/10.1021/acsearthspacechem.2c00054>.

Concentration of metal elements; concentration of PAHs; spectral irradiance of the UV–vis light; and results of blank experiments (PDF)

## ■ AUTHOR INFORMATION

### Corresponding Authors

Liubin Huang – Environment Research Institute, Shandong University, Qingdao 266237 Shandong, China; Email: [hliubin@sdu.edu.cn](mailto:hliubin@sdu.edu.cn)

Likun Xue – Environment Research Institute, Shandong University, Qingdao 266237 Shandong, China; [orcid.org/0000-0001-7329-2110](https://orcid.org/0000-0001-7329-2110); Email: [xuelikun@sdu.edu.cn](mailto:xuelikun@sdu.edu.cn)

Wenxing Wang – Environment Research Institute, Shandong University, Qingdao 266237 Shandong, China; Email: [wxxwang@sdu.edu.cn](mailto:wxxwang@sdu.edu.cn)

### Authors

Chuan Yu – Environment Research Institute, Shandong University, Qingdao 266237 Shandong, China

Hengqing Shen – Environment Research Institute, Shandong University, Qingdao 266237 Shandong, China

Zeyuan Li – Focused Photonics (Hangzhou) Inc., Hangzhou 310052 Zhejiang, China

Min Zhao – Environment Research Institute, Shandong University, Qingdao 266237 Shandong, China

Juan Yang – Environment Research Institute, Shandong University, Qingdao 266237 Shandong, China

Yingnan Zhang – Environment Research Institute, Shandong University, Qingdao 266237 Shandong, China

Hongyong Li – Environment Research Institute, Shandong University, Qingdao 266237 Shandong, China

Jiangshan Mu – Environment Research Institute, Shandong University, Qingdao 266237 Shandong, China

Complete contact information is available at:

<https://pubs.acs.org/10.1021/acsearthspacechem.2c00054>



## Notes

The authors declare no competing financial interest.

## ACKNOWLEDGMENTS

This work was funded by the National Natural Science Foundation of China (Grant Nos. 41922051 and 42061160478) and the Jiangsu Collaborative Innovation Center for Climate Change.

## REFERENCES

- (1) Acker, K.; Möller, D.; Wieprecht, W.; Meixner, F. X.; Bohn, B.; Gilge, S.; Plass-Dülmer, C.; Berresheim, H. Strong Daytime Production of OH from HNO<sub>2</sub> at a Rural Mountain Site. *Geophys. Res. Lett.* **2006**, *33*, No. L02809.
- (2) Kleffmann, J. Daytime Sources of Nitrous Acid (HONO) in the Atmospheric Boundary Layer. *ChemPhysChem* **2007**, *8*, 1137–1144.
- (3) Xue, L. K.; Wang, T.; Zhang, J. M.; Zhang, X. C.; Deliger, Poon, C. N.; Ding, A. J.; Zhou, X. H.; Wu, W. S.; Tang, J.; et al. Source of Surface Ozone and Reactive Nitrogen Speciation at Mount Waliguan in Western China: New Insights from the 2006 Summer Study. *J. Geophys. Res.* **2011**, *116*, No. D07306.
- (4) Fu, X.; Wang, T.; Zhang, L.; Li, Q.; Wang, Z.; Xia, M.; Yun, H.; Wang, W.; Yu, C.; Yue, D.; et al. The Significant Contribution of HONO to Secondary Pollutants during a Severe Winter Pollution Event in Southern China. *Atmos. Chem. Phys.* **2019**, *19*, 1–14.
- (5) Pagsberg, P.; Bjergbakke, E.; Ratajczak, E.; Sillesen, A. Kinetics of the Gas Phase Reaction OH + NO(+M) → HONO(+M) and the Determination of the UV Absorption Cross Sections of HONO. *Chem. Phys. Lett.* **1997**, *272*, 383–390.
- (6) Kleffmann, J.; Becker, K. H.; Wiesen, P. Heterogeneous NO<sub>2</sub> Conversion Processes on Acid Surfaces: Possible Atmospheric Implications. *Atmos. Environ.* **1998**, *32*, 2721–2729.
- (7) Finlayson-Pitts, B. J.; Wingen, L. M.; Sumner, A. L.; Syomin, D.; Ramazan, K. A. The Heterogeneous Hydrolysis of NO<sub>2</sub> in Laboratory Systems and in Outdoor and Indoor Atmospheres: An Integrated Mechanism. *Phys. Chem. Chem. Phys.* **2003**, *5*, 223–242.
- (8) Stutz, J.; Alicke, B.; Ackermann, R.; Geyer, A.; Wang, S.; White, A. B.; Williams, E. J.; Spicer, C. W.; Fast, J. D. Relative Humidity Dependence of HONO Chemistry in Urban Areas. *J. Geophys. Res.* **2004**, *109*, No. D03307.
- (9) Acker, K.; Möller, D.; Wieprecht, W.; Meixner, F. X.; Bohn, B.; Gilge, S.; Plass-Dülmer, C.; Berresheim, H. Strong Daytime Production of OH from HNO<sub>2</sub> at a Rural Mountain Site. *Geophys. Res. Lett.* **2006**, *33*, No. L02809.
- (10) Sörgel, M.; Regelin, E.; Bozem, H.; Diesch, J. M.; Drewnick, F.; Fischer, H.; Harder, H.; Held, A.; Hosaynali-Beygi, Z.; Martinez, M.; et al. Quantification of the Unknown HONO Daytime Source and its Relation to NO<sub>2</sub>. *Atmos. Chem. Phys.* **2011**, *11*, 10433–10447.
- (11) Zhou, X.; Gao, H.; He, Y.; Huang, G.; Bertman, S. B.; Civerolo, K.; Schwab, J. Nitric Acid Photolysis on Surfaces in Low-NO<sub>x</sub> Environments: Significant Atmospheric Implications. *Geophys. Res. Lett.* **2003**, *30*, No. 2217.
- (12) Laufs, S.; Kleffmann, J. Investigations on HONO Formation from Photolysis of Adsorbed HNO<sub>3</sub> on Quartz Glass Surfaces. *Phys. Chem. Chem. Phys.* **2016**, *18*, 9616–9625.
- (13) Baergen, A. M.; Donaldson, D. J. Photochemical Renoxification of Nitric Acid on Real Urban Grime. *Environ. Sci. Technol.* **2013**, *47*, 815–820.
- (14) Ye, C.; Gao, H.; Zhang, N.; Zhou, X. Photolysis of Nitric Acid and Nitrate on Natural and Artificial Surfaces. *Environ. Sci. Technol.* **2016**, *50*, 3530–3536.
- (15) Stemmler, K.; Ammann, M.; Donders, C.; Kleffmann, J.; George, C. Photosensitized Reduction of Nitrogen Dioxide on Humic Acid as a Source of Nitrous Acid. *Nature* **2006**, *440*, 195–198.
- (16) Stemmler, K.; Ndour, M.; Elshorbany, Y.; Kleffmann, J.; D'anna, B.; George, C.; Bohn, B.; Ammann, M. Light Induced Conversion of Nitrogen Dioxide into Nitrous Acid on Submicron Humic Acid Aerosol. *Atmos. Chem. Phys.* **2007**, *7*, 4237–4248.
- (17) Han, C.; Yang, W.; Wu, Q.; Yang, H.; Xue, X. Heterogeneous Photochemical Conversion of NO<sub>2</sub> to HONO on the Humic Acid Surface under Simulated Sunlight. *Environ. Sci. Technol.* **2016**, *50*, 5017–5023.
- (18) George, C.; Streckowski, R. S.; Kleffmann, J.; Stemmler, K.; Ammann, M. Photoenhanced Uptake of Gaseous NO<sub>2</sub> on Solid-Organic Compounds: A Photochemical Source of HONO? *Faraday Discuss.* **2005**, *130*, 195–210.
- (19) Brigante, M.; Cazor, D.; D'Anna, B.; George, C.; Donaldson, D. J. Photoenhanced Uptake of NO<sub>2</sub> by Pyrene Solid Films. *J. Phys. Chem. A* **2008**, *112*, 9503–9508.
- (20) Ammar, R.; Monge, M. E.; George, C.; D'Anna, B. Photoenhanced NO<sub>2</sub> Loss on Simulated Urban Grime. *ChemPhysChem* **2010**, *11*, 3956–3961.
- (21) Cazor, D.; Brigante, M.; Ammar, R.; D'Anna, B.; George, C. Heterogeneous Photochemistry of Gaseous NO<sub>2</sub> on Solid Fluoranthene Films: A Source of Gaseous Nitrous Acid (HONO) in the Urban Environment. *J. Photochem. Photobiol. A* **2014**, *273*, 23–28.
- (22) Ndour, M.; D'Anna, B.; George, C.; Ka, O.; Balkanski, Y.; Kleffmann, J.; Stemmler, K.; Ammann, M. Photoenhanced Uptake of NO<sub>2</sub> on Mineral Dust: Laboratory Experiments and Model Simulations. *Geophys. Res. Lett.* **2008**, *35*, No. L05812.
- (23) Ndour, M.; Nicolas, M.; D'Anna, B.; Ka, O.; George, C. Photoreactivity of NO<sub>2</sub> on Mineral Dusts Originating from Different Locations of the Sahara Desert. *Phys. Chem. Chem. Phys.* **2009**, *11*, 1312–1319.
- (24) Dupart, Y.; Fine, L.; D'Anna, B.; George, C. Heterogeneous Uptake of NO<sub>2</sub> on Arizona Test Dust under UV-A Irradiation: An Aerosol Flow Tube Study. *Aeolian Res.* **2014**, *15*, 45–51.
- (25) Monge, M. E.; D'Anna, B.; George, C. Nitrogen Dioxide Removal and Nitrous Acid Formation on Titanium Oxide Surfaces—An Air Quality Remediation Process? *Phys. Chem. Chem. Phys.* **2010**, *12*, 8991–8998.
- (26) Monge, M. E.; D'Anna, B.; Mazri, L.; Giroir-Fendler, A.; Ammann, M.; Donaldson, D. J.; George, C. Light Changes the Atmospheric Reactivity of Soot. *Proc. Natl. Acad. Sci. U.S.A.* **2010**, *107*, 6605–6609.
- (27) Liu, J.; Deng, H.; Li, S.; Jiang, H.; Mekic, M.; Zhou, W.; Wang, Y.; Loisel, G.; Wang, X.; Gligorovski, S. Light-Enhanced Heterogeneous Conversion of NO<sub>2</sub> to HONO on Solid Films Consisting of Fluorene and Fluorene/Na<sub>2</sub>SO<sub>4</sub>: An Impact on Urban and Indoor Atmosphere. *Environ. Sci. Technol.* **2020**, *54*, 11079–11086.
- (28) Guan, C.; Li, X.; Luo, Y.; Huang, Z. Heterogeneous Reaction of NO<sub>2</sub> on α-Al<sub>2</sub>O<sub>3</sub> in the Dark and Simulated Sunlight. *J. Phys. Chem. A* **2014**, *118*, 6999–7006.
- (29) Yu, C.; Wang, Z.; Ma, Q.; Xue, L.; George, C.; Wang, T. Measurement of Heterogeneous Uptake of NO<sub>2</sub> on Inorganic Particles, Sea Water and Urban Grime. *J. Environ. Sci.* **2021**, *106*, 124–135.
- (30) Han, C.; Yang, W.; Yang, H.; Xue, X. Enhanced Photochemical Conversion of NO<sub>2</sub> to HONO on Humic Acids in the Presence of Benzophenone. *Environ. Pollut.* **2017**, *231*, 979–986.
- (31) Diamond, M. L.; Gingrich, S. E.; Fertuck, K.; McCarry, B. E.; Stern, G. A.; Billeck, B.; Grift, B.; Brooker, D.; Yager, T. D. Evidence for Organic Film on an Impervious Urban Surface: Characterization and Potential Teratogenic Effects. *Environ. Sci. Technol.* **2000**, *34*, 2900–2908.
- (32) Lam, B.; Diamond, M. L.; Simpson, A. J.; Makar, P. A.; Truong, J.; Hernandez-Martinez, N. A. Chemical Composition of Surface Films on Glass Windows and Implications for Atmospheric Chemistry. *Atmos. Environ.* **2005**, *39*, 6578–6586.
- (33) Simpson, A. J.; Lam, B.; Diamond, M. L.; Donaldson, D. J.; Lefebvre, B. A.; Moser, A. Q.; Williams, A. J.; Larin, N. I.; Kvasha, M. P. Assessing the Organic Composition of Urban Surface Films using Nuclear Magnetic Resonance Spectroscopy. *Chemosphere* **2006**, *63*, 142–152.
- (34) Wu, R. W.; Harner, T.; Diamond, M. L. Evolution Rates and PCB Content of Surface Films that Develop on Impervious Urban Surfaces. *Atmos. Environ.* **2008**, *42*, 6131–6143.

- (35) Lombardo, T.; Chabas, A.; Verney-Carron, A.; Cachier, H.; Triquet, S.; Darchy, S. Physico-Chemical Characterisation of Glass Soiling in Rural, Urban and Industrial Environments. *Environ. Sci. Pollut. Res.* **2014**, *21*, 9251–9258.
- (36) Diamond, M. L.; Priemer, D. A.; Law, N. L. Developing a Multimedia Model of Chemical Dynamics in an Urban Area. *Chemosphere* **2001**, *44*, 1655–1667.
- (37) Csiszar, S. A.; Diamond, M. L.; Thibodeaux, L. J. Modeling Urban Films Using a Dynamic Multimedia Fugacity Model. *Chemosphere* **2012**, *87*, 1024–1031.
- (38) Liu, J.; Li, S.; Mekic, M.; Jiang, H.; Zhou, W.; Loisel, G.; Song, W.; Wang, X.; Gligorovski, S. Photoenhanced Uptake of NO<sub>2</sub> and HONO Formation on Real Urban Grime. *Environ. Sci. Technol. Lett.* **2019**, *6*, 413–417.
- (39) Liu, Q.-T.; Chen, R.; McCarry, B. E.; Diamond, M. L.; Bahavar, B. Characterization of Polar Organic Compounds in the Organic Film on Indoor and Outdoor Glass Windows. *Environ. Sci. Technol.* **2003**, *37*, 2340–2349.
- (40) Butt, C. M.; Diamond, M. L.; Truong, J.; Ikonou, M. G.; Ter Schure, A. F. Spatial Distribution of Polybrominated Diphenyl Ethers in Southern Ontario as Measured in Indoor and Outdoor Window Organic Films. *Environ. Sci. Technol.* **2004**, *38*, 724–731.
- (41) Baergen, A. M.; Styler, S. A.; van Pinxteren, D.; Muller, K.; Herrmann, H.; Donaldson, D. J. Chemistry of Urban Grime: Inorganic Ion Composition of Grime vs Particles in Leipzig, Germany. *Environ. Sci. Technol.* **2015**, *49*, 12688–12696.
- (42) Styler, S. A.; Baergen, A. M.; Donaldson, D. J.; Herrmann, H. Organic Composition, Chemistry, and Photochemistry of Urban Film in Leipzig, Germany. *ACS Earth Space Chem.* **2018**, *2*, 935–945.
- (43) Baergen, A. M.; Donaldson, D. J. Seasonality of the Water-Soluble Inorganic Ion Composition and Water Uptake Behavior of Urban Grime. *Environ. Sci. Technol.* **2019**, *53*, 5671–5677.
- (44) Kropitavich, C. R.; Zhou, S.; Kowal, S. F.; Kahan, T. F. Physical and Chemical Characterization of Urban Grime Sampled from Two Cities. *ACS Earth Space Chem.* **2020**, *4*, 1813–1822.
- (45) DeYoung, J. L.; Holyoake, E. A.; Shaw, S. K. What Are the Differences between Two Environmental Films Sampled 1 km Apart? *ACS Earth Space Chem.* **2021**, *5*, 3407–3413.
- (46) Li, D.; Xue, L.; Wen, L.; Wang, X.; Chen, T.; Mellouki, A.; Chen, J.; Wang, W. Characteristics and Sources of Nitrous Acid in an Urban Atmosphere of Northern China: Results from 1-yr Continuous Observations. *Atmos. Environ.* **2018**, *182*, 296–306.
- (47) Wen, L.; Chen, T.; Zheng, P.; Wu, L.; Wang, X.; Mellouki, A.; Xue, L.; Wang, W. Nitrous Acid in Marine Boundary Layer over Eastern Bohai Sea, China: Characteristics, Sources, and Implications. *Sci. Total Environ.* **2019**, *670*, 282–291.
- (48) Jiang, Y.; Xue, L.; Gu, R.; Jia, M.; Zhang, Y.; Wen, L.; Zheng, P.; Chen, T.; Li, H.; Shan, Y.; et al. Sources of Nitrous Acid (HONO) in the Upper Boundary Layer and Lower Free Troposphere of the North China Plain: Insights from the Mount Tai Observatory. *Atmos. Chem. Phys.* **2020**, *20*, 12115–12131.
- (49) Gu, R.; Zheng, P.; Chen, T.; Dong, C.; Wang, Y.; Liu, Y.; Liu, Y.; Luo, Y.; Han, G.; Wang, X.; et al. Atmospheric Nitrous Acid (HONO) at a Rural Coastal Site in North China: Seasonal Variations and Effects of Biomass Burning. *Atmos. Environ.* **2020**, *229*, No. 117429.
- (50) Yang, J.; Shen, H.; Guo, M.-Z.; Zhao, M.; Jiang, Y.; Chen, T.; Liu, Y.; Li, H.; Zhu, Y.; Meng, H.; et al. Strong Marine-Derived Nitrous Acid (HONO) Production Observed in the Coastal Atmosphere of Northern China. *Atmos. Environ.* **2021**, *244*, No. 117948.
- (51) Heland, J.; Kleffmann, J.; Kurtenbach, R.; Wiesen, P. A New Instrument to Measure Gaseous Nitrous Acid (HONO) in the Atmosphere. *Environ. Sci. Technol.* **2001**, *35*, 3207–3212.
- (52) Gustafsson, R. J.; Orlov, A.; Griffiths, P. T.; Cox, R. A.; Lambert, R. M. Reduction of NO<sub>2</sub> to Nitrous Acid on Illuminated Titanium Dioxide Aerosol Surfaces: Implications for Photocatalysis and Atmospheric Chemistry. *Chem. Commun.* **2006**, *37*, 3936–3938.
- (53) Langridge, J. M.; Gustafsson, R. J.; Griffiths, P. T.; Cox, R. A.; Lambert, R. M.; Jones, R. L. Solar Driven Nitrous Acid Formation on Building Material Surfaces Containing Titanium Dioxide: A Concern for Air Quality in Urban Areas? *Atmos. Environ.* **2009**, *43*, 5128–5131.
- (54) Baltrusaitis, J.; Jayaweera, P. M.; Grassian, V. H. XPS Study of Nitrogen Dioxide Adsorption on Metal Oxide Particle Surfaces under Different Environmental Conditions. *Phys. Chem. Chem. Phys.* **2009**, *11*, 8295–8305.
- (55) Bedjanian, Y.; El Zein, A. Interaction of NO<sub>2</sub> with TiO<sub>2</sub> Surface under UV Irradiation: Products Study. *J. Phys. Chem. A* **2012**, *116*, 1758–1764.
- (56) Chen, H.; Nanayakkara, C. E.; Grassian, V. H. Titanium Dioxide Photocatalysis in Atmospheric Chemistry. *Chem. Rev.* **2012**, *112*, 5919–5948.
- (57) Gao, X.; Gao, W.; Sun, X.; Jiang, W.; Wang, Z.; Li, W. Measurements of Indoor and Outdoor Fine Particulate Matter during the Heating Period in Jinan, in North China: Chemical Composition, Health Risk, and Source Apportionment. *Atmosphere* **2020**, *11*, 885.
- (58) Chen, R.; Cheng, J.; Lv, J.; Wu, L.; Wu, J. Comparison of Chemical Compositions in Air Particulate Matter during Summer and Winter in Beijing, China. *Environ. Geochem. Health* **2017**, *39*, 913–921.
- (59) Huang, L.; Wang, G. Chemical Characteristics and Source Apportionment of Atmospheric Particles during Heating Period in Harbin, China. *J. Environ. Sci.* **2014**, *26*, 2475–2483.
- (60) Kong, S.; Ji, Y.; Lu, B.; Bai, Z.; Chen, L.; Han, B.; Li, Z. Chemical Compositions and Sources of Atmospheric PM<sub>10</sub> in Heating, Non-Heating and Sand Periods at a Coal-Based City in Northeastern China. *J. Environ. Monit.* **2012**, *14*, 852–865.
- (61) Hu, R.; Liu, G.; Zhang, H.; Xue, H.; Wang, X.; Wang, R. Particle-Associated Polycyclic Aromatic Hydrocarbons (PAHs) in the Atmosphere of Hefei, China: Levels, Characterizations and Health Risks. *Arch. Environ. Contam. Toxicol.* **2018**, *74*, 442–451.
- (62) Zhou, C.; Zhu, X.; Wang, Z.; Ma, X.; Chen, J.; Ni, Y.; Wang, W. E. I.; Mu, J. U. N.; Li, X. Gas-Particle Partitioning of PAHs In The Urban Air of Dalian, China: Measurements and Assessments. *Polycycl. Aromatic Compd.* **2013**, *33*, 31–51.
- (63) Okuda, T.; Naoi, D.; Tenmoku, M.; Tanaka, S.; He, K.; Ma, Y.; Yang, F.; Lei, Y.; Jia, Y.; Zhang, D. Polycyclic Aromatic Hydrocarbons (PAHs) in the Aerosol in Beijing, China, Measured by Amino-propylsilane Chemically-Bonded Stationary-Phase Column Chromatography and HPLC/Fluorescence Detection. *Chemosphere* **2006**, *65*, 427–435.
- (64) Wu, S.-P.; Tao, S.; Zhang, Z.-H.; Lan, T.; Zuo, Q. Distribution of Particle-Phase Hydrocarbons, PAHs and OCPs in Tianjin, China. *Atmos. Environ.* **2005**, *39*, 7420–7432.
- (65) Ellshorbany, Y. F.; Kurtenbach, R.; Wiesen, P.; Lissi, E.; Rubio, M.; Villena, G.; Gramsch, E.; Rickard, A. R.; Pilling, M. J.; Kleffmann, J. Oxidation Capacity of the City Air of Santiago, Chile. *Atmos. Chem. Phys.* **2009**, *9*, 2257–2273.
- (66) Tang, Y.; An, J.; Wang, F.; Li, Y.; Qu, Y.; Chen, Y.; Lin, J. Impacts of an Unknown Daytime HONO Source on the Mixing Ratio and Budget of HONO, and Hydroxyl, Hydroperoxyl, and Organic Peroxy Radicals, in the Coastal Regions of China. *Atmos. Chem. Phys.* **2015**, *15*, 9381–9398.
- (67) Spataro, F.; Ianniello, A.; Esposito, G.; Allegrini, I.; Zhu, T.; Hu, M. Occurrence of Atmospheric Nitrous Acid in the Urban Area of Beijing (China). *Sci. Total Environ.* **2013**, *447*, 210–224.
- (68) Vogel, B.; Vogel, H.; Kleffmann, J.; Kurtenbach, R. Measured and Simulated Vertical Profiles of Nitrous Acid—Part II. Model Simulations and Indications for a Photolytic Source. *Atmos. Environ.* **2003**, *37*, 2957–2966.
- (69) Li, G.; Lei, W.; Zavala, M.; Volkamer, R.; Dusanter, S.; Stevens, P.; Molina, L. T. Impacts of HONO Sources on the Photochemistry in Mexico City during the MCMA-2006/MILAGO Campaign. *Atmos. Chem. Phys.* **2010**, *10*, 6551–6567.
- (70) Zhang, L.; Wang, T.; Zhang, Q.; Zheng, J.; Xu, Z.; Lv, M. Potential Sources of Nitrous Acid (HONO) and Their Impacts on



Ozone: A WRF-Chem Study in a Polluted Subtropical Region. *J. Geophys. Res.* **2016**, *121*, 3645–3662.

### NOTE ADDED AFTER ASAP PUBLICATION

This paper was published ASAP on June 24, 2022, where the unit of S/V was used as “/dm” during the calculation of uptake coefficient throughout the paper. This error was corrected, and the updated version was reposted on July 23, 2022.

## Recommended by ACS

### Photolysis of Nitroaromatic Compounds under Sunlight: A Possible Daytime Photochemical Source of Nitrous Acid?

Wangjin Yang, Xiangxin Xue, *et al.*

AUGUST 17, 2021  
ENVIRONMENTAL SCIENCE & TECHNOLOGY LETTERS

READ 

### Impact of Tetrabutylammonium on the Oxidation of Bromide by Ozone

Shuzhen Chen, Markus Ammann, *et al.*

OCTOBER 26, 2021  
ACS EARTH AND SPACE CHEMISTRY

READ 

### Ozonolysis of Oleic Acid Aerosol Revisited: Multiphase Chemical Kinetics and Reaction Mechanisms

Thomas Berkemeier, Ulrich Pöschl, *et al.*

NOVEMBER 19, 2021  
ACS EARTH AND SPACE CHEMISTRY

READ 

### Effects of Acidity on Reactive Oxygen Species Formation from Secondary Organic Aerosols

Jinlai Wei, Manabu Shiraiwa, *et al.*

APRIL 29, 2022  
ACS ENVIRONMENTAL AU

READ 

Get More Suggestions >